DIAGNOSTIC NUCLEAR MEDICINE

Single-Photon Emission Computed Tomography (SPECT) for Assessment of Hepatic Lesions

Ludwig Strauss, Frank Bostel, John H. Clorius, Ekaterini Raptou, Henry Wellman, and Peter Georgi

German Cancer Research Center, Heidelberg, Germany

Single-photon emission computed tomography (SPECT) and conventional scintigraphy were compared in 130 patients examined to assess hepatic involvement in malignant disease. Transmission computed tomography (TCT) served as the reference method against which SPECT and conventional scintigraphy were compared. The sensitivity of SPECT was calculated for lesions grouped according to diameter as well as location. The Bayesian theorem was used to assess the reliability of both SPECT and conventional scintigraphy. SPECT identified only 52% of lesions with a diameter of 1.5–2.0 cm. It was also shown that the sensitivity of SPECT was lowest for small lesions in the middle third of the liver. A comparison of the final diagnosis demonstrated that SPECT had greater sensitivity, specificity, and accuracy than conventional scans, and is superior at low disease prevalence. At high disease prevalence, SPECT has a lower rate of false negatives. SPECT appears to be the superior imaging modality for evaluation of the liver in malignant disease.

J Nucl Med 23: 1059–1065, 1982

One of the basic procedures in tumor staging includes the diagnostic evaluation of the liver to identify possible hepatic involvement. Transmission computed tomography (TCT), ultrasound, and conventional scintigrams are used extensively in the hepatic evaluation of malignant disease (*1–3*). TCT is reported to be the most sensitive, specific, and accurate of these methods (*4–6*). SPECT can be expected to find extensive use in liver scintigraphy, particularly since the theoretical lesion detectibility is superior to that of conventional scintigraphy (*7–9*).

The present study was performed to assess the lesion detectibility of SPECT in metastatic liver disease by comparing results obtained from this procedure with those of conventional scintigrams, using transmission computed tomography (TCT) as the reference procedure. The results of the study were then examined with Bayesian analysis to determine the utility of standard scintigraphy and SPECT at different prevalences of disease.

Received Dec. 23, 1981; revision accepted Aug. 4, 1982.

For reprints contact: Ludwig Strauss, Institute of Clinical Radiology, Klinikum Mannheim, Theodor-Kutzer-Ufer, D-6800 Mannheim, West-Germany.

METHODS

The study contains 145 patients referred for liver scintigraphy for tumor staging or restaging under chemotherapy. The majority of patients included in the study had bronchogenic carcinoma, followed by carcinoma of the breast, and gastrointestinal tumors (Table 1).

Liver scintigraphy followed i.v. injection of 4 mCi Tc-99m tin colloid. Conventional scintigrams were obtained before the tomographic images. A large-field-of-view conventional gamma camera equipped with a high-resolution parallel-hole collimator was used for both examinations. We used a 20% window centered at 140 keV. The camera was interfaced to a minicomputer system. Each image contained 1,000,000 counts. Con-

TABLE 1. PRIMARY TUMORS OF 130 PATIENTS EXAMINED WITH CONVENTIONAL SCINTIGRAPHY, SPECT AND TCT

Primary tumors	Frequency	
	(%)	(n)
Bronchogenic malignancy	75	98
Gastrointestinal tumors	19	25
Carcinoma of the breast	4	5
Bladder carcinoma	1	1
Hypernephroma	1	1
Total	100	130

ventional images were acquired in anterior, posterior, and right lateral positions. When initial scans appeared equivocal, the sequence of images was expanded to include left lateral and upright scans. Immediately following conventional scintigraphy, and without repeat radiotracer injection, we obtained SPECT images. During this examination, the single camera orbits in a circle around the patient. Images were made at 64 equal angular intervals. The average count rate was in excess of 150,000 counts per image. This required approximately 30 min of scan time. We use the SPECT software developed at the Karolinska Institute for the reconstruction of transverse slices (*8*). The theoretical transverse-section thickness can be 0.625, 1.25, or 1.875 cm. Coronal, sagittal, and oblique sections can be derived from the transverse sections. SPECT images were evaluated by two experienced observers.

The TCT examination was always obtained within four weeks of the liver scintigram. TCT was used as the reference method against which conventional scintigraphy and SPECT were compared. A fast fan-beam scanner with a scanning and reconstruction time of 5 sec was used. The liver was initially examined, without contrast-medium enhancement, in slices 8 mm thick. When required, the examination was continued following infusion of 75 g diatrizoate meglumine in a 250-ml volume. All lesions were identified on the initial scan. Contrast enhancement, however, served to assess vascularity and to help deliniate the border of the lesion. An off-line diagnostic terminal was used to determine the diameter of visualized lesions. When defects were irregular, the largest measured diameter was registered. Lesions were classified in nine groups according to diameter, beginning at one cm and advancing to 5.5 cm. Patients were excluded from the study if fatty infiltration and/or inhomogeneous normal liver tissue was identified. Fifteen examinations were excluded for this reason. Thus conventional scintigrams, SPECT, and TCT from 130 patients were available for the comparisons.

The final evaluation was carried out in four steps.

1. The final diagnosis reached with single-photon emission computed tomography was compared with

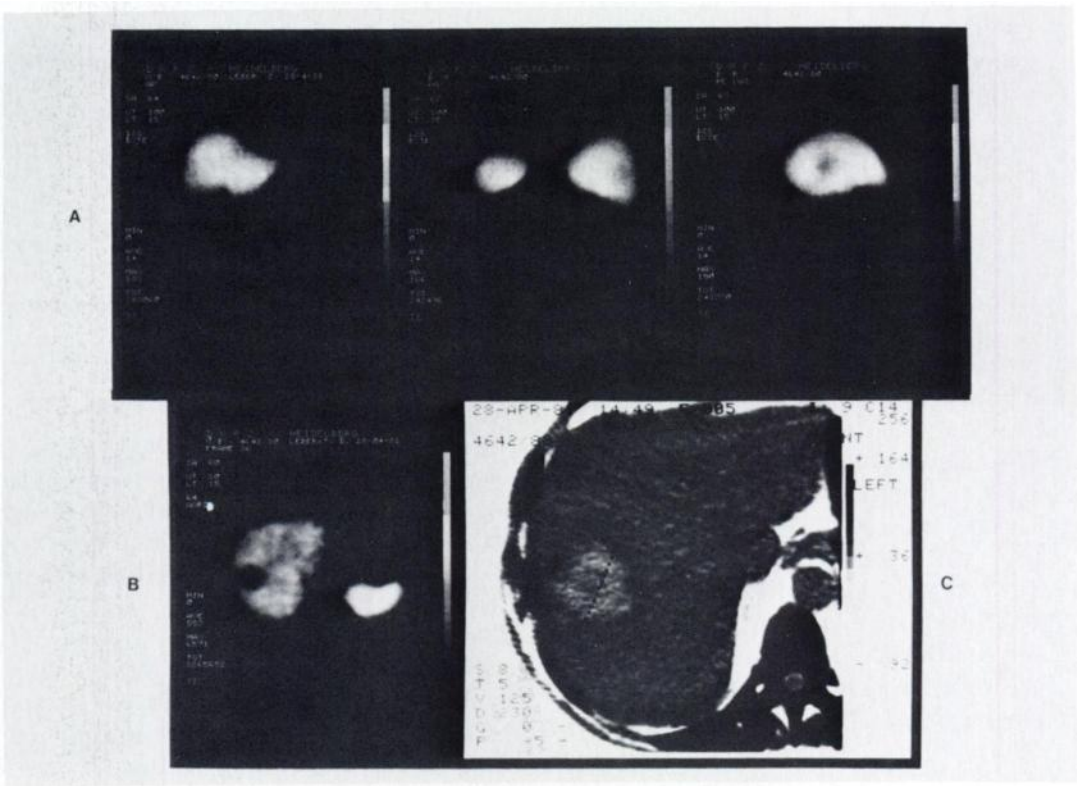

FIG. 1. A (top row): Conventional scintigrams in anterior, posterior, and right lateral view. B (bottom row, left): Single-photon emission computed tomography, transverse slice. C (bottom row, right) Portion of TCT slice showing the 4.2-cm metastasis. All imaging procedures demonstrated defect in right lateral part of liver.

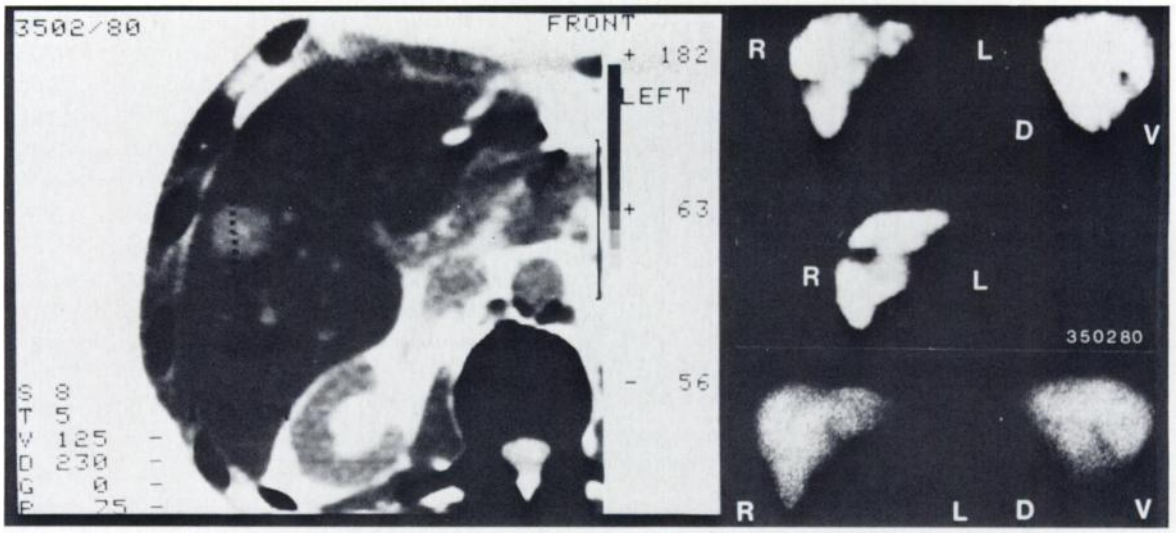

FIG. 2. Left: TCT slice showing 1.9-cm metastasis. This mass was clearly seen only in TCT and SPECT images. Bottom row, right: Conventional anterior and right lateral scintigrams. Middle row, right: Single-photon emission computed tomography, transverse slice. Top row, right: Reconstructed frontal and sagittal SPECT views.

results obtained with conventional imaging. Both results were compared against TCT, the reference method. Sensitivity, specificity, and accuracy were calculated for each procedure.

2. Lesions were classified according to their diameter. SPECT images were examined to identify those lesions seen in TCT.

3. Lesions were classified according to location and size. Lesions with different diameters identified in TCT were grouped according to location as being in the right, middle, or left third of the liver. The sensitivity of SPECT was calculated for every group.

4. The Bayesian theorem was used to grade the information given by a diagnostic procedure at different levels of prevalence of metastases (*10–12*).

RESULTS

Larger-sized lesions were generally visualized with all imaging modalities (Fig. 1). In comparison with conventional scintigrams, SPECT offers topographic defect portrayal similar to that of TCT. Small-diameter lesions were recognized more frequently with SPECT than with conventional scintigraphy (Fig. 2). To assess lesion detectability of SPECT and conventional scans, we compared both procedures with the results achieved with TCT.

SPECT and conventional scintigrams were at hand for 130 patients. In 77 of the 130 patients, TCT demonstrated metastases of the liver (Table 2). The true-positive ratio for SPECT, using TCT as reference, was 94%. In comparison, conventional imaging yielded a ratio of only 81%. The accuracy of SPECT was found to be 92%, whereas that of conventional scintigraphy was 82%.

Sixty-five patients had 156 liver metastases by TCT. Lesions were placed into one of nine groups according

TABLE 2. DECISION MATRIX FOR SPECT (2a) AND CONVENTIONAL LIVER SCANS (2b). THE EVALUATION INCLUDES 130 PATIENTS IN WHOM TCT SERVED AS REFERENCE METHOD

2a			
Spect results	TCT results		
	Abnormal	Normal	Total
Abnormal	72	6	78
Normal	5	47	52
Total	77	53	130

True positives = (72/77) · 100 = 94%
True negatives = (47/53) · 100 = 89%
False positives = (6/53) · 100 = 11%
False negatives = (5/77) · 100 = 6%
Accuracy = ((72 + 47)/130) · 100 = 92%

2b			
Conventional Scintigraphic results	TCT results		
	Abnormal	Normal	Total
Abnormal	62	8	70
Normal	15	45	60
Total	77	53	130

True positives = (62/77) · 100 = 81%
True negatives = (45/53) · 100 = 85%
False positives = (8/53) · 100 = 15%
False negatives = (15/77) · 100 = 19%
Accuracy = ((62 + 45)/130) · 100 = 82%

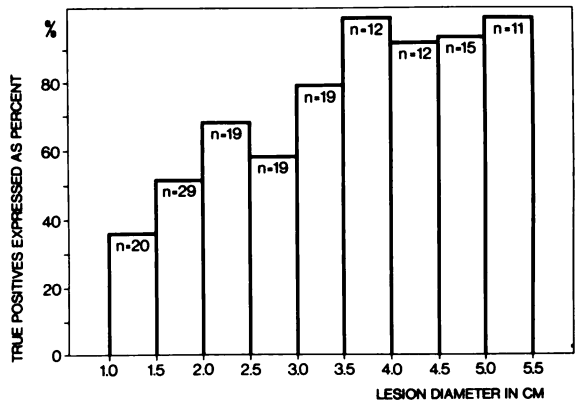

FIG. 3. True-positive results of SPECT examinations in 65 patients who had 156 hepatic lesions. TCT served as reference method and was used to determine diameters of lesions.

to size (Fig. 3). The sensitivity of SPECT was found to be 35% for metastases having a diameter of 1.0–1.5 cm, progressing to 52% for lesions of 1.5–2.0 cm (Fig. 3). Sensitivity reached 68% for metastases with a diameter of 2.0–2.5 cm. A true-positive value exceeding 90% was observed in groups having a diameter above 3.5 cm.

One hundred and forty-five metastases seen by TCT, having a diameter of one to five cm, were classified according to both size and location. Eleven metastases, each with a diameter above 5 cm, were excluded from the evaluation. Sixty-seven percent of all lesions localized in the right-hand third of the liver, and having a diameter of 2–3 cm, were identified with SPECT (Table 3). The location of hepatic lesions clearly influenced recognition with SPECT. The rate of true positives was lowest in the middle section of the liver, when the organ was divided equally into three parts. A lesion diameter of 2–3 cm was associated with a true-positive rate of 56%, while for a true-positive rate of 80%, lesions required a diameter of at least 3 cm (Fig. 3). Indeed, one lesion with a 4–5 cm diameter was missed in the middle third of the liver beneath the hilus.

The Bayesian theorem was applied to our data, as demonstrated in Table 2 and Fig. 4. At 20% disease prevalence, the posterior probability of obtaining a false-negative result with SPECT was below 2%, and at 80% prevalence it was 21% (Fig. 4). In comparison, conventional scans had a posterior probability of false-negative results of 5% at 20% disease prevalence, and of 47% at 80% prevalence (Fig. 4). Furthermore, the Bayesian theorem indicates that the posterior probability of true-positives with SPECT is 68% at 20% disease prevalence, and at 80% probability of disease the posterior probability of true-positives is 97% (Fig. 4). In comparison, conventional liver imaging would be expected to have a 'true-positive' posterior probability of 57% at a 20% disease rate and 96% at 80% disease occurrence (Fig. 4).

If a diagnostic procedure gives no additional information, the prior and posterior probabilities of visualizing metastases would be equal. The plot would be a straight line (Fig. 4). Every additional bit of information obtained with the diagnostic procedure would raise the posterior probability of reaching a correct diagnosis. The discriminant function is the difference between the posterior probability of a true-positive (curves 1 and 3 in Fig. 4) and false-negative diagnosis (curves 2 and 4 in Fig. 4). One can characterize the power of the tested procedure by using the discriminant function. When the power of conventional imaging was compared with SPECT, we found SPECT imaging to be superior for every prevalence of disease (Fig. 5). The maximum discriminant value of SPECT as calculated with formula 4d (see Appendix), was 84% at 57% prior probability of disease. For conventional scintigraphy it was 66% at 48% prior probability of metastases.

DISCUSSION

TCT is reported to be the most sensitive, specific, and accurate imaging procedure in the evaluation of the liver in malignant disease (*4–6*). Only 52% of the focal hepatic defects with a diameter of 1.5–2.0 cm were visualized with SPECT. Scherer et al. reported that the sensitivity of TCT for lesions of this size is 90% (*13*). Their study was performed in vitro, so the in-vivo values might be somewhat lower. It does appear, however, that the spatial resolution of TCT is significantly better compared with that of SPECT.

TABLE 3. INFLUENCE OF LOCALIZATION AND SIZE OF HEPATIC LESIONS ON SPECT SENSITIVITY IN 65 PATIENTS WITH 145 METASTASES. EXCLUDED ARE MASSES EXCEEDING 5 CM IN DIAMETER. RESULTS ARE GIVEN IN ABSOLUTE NUMBERS

Diameter	Liver divided into three equal parts					
	Right section		Middle section		Left section	
cm	True positive	Total	True positive	Total	True positive	Total
1 < 2	19	36	2	11	2	3
2 < 3	16	24	5	9	3	5
3 < 4	17	18	7	9	3	4
4 < 5	12	12	12	13	0	1

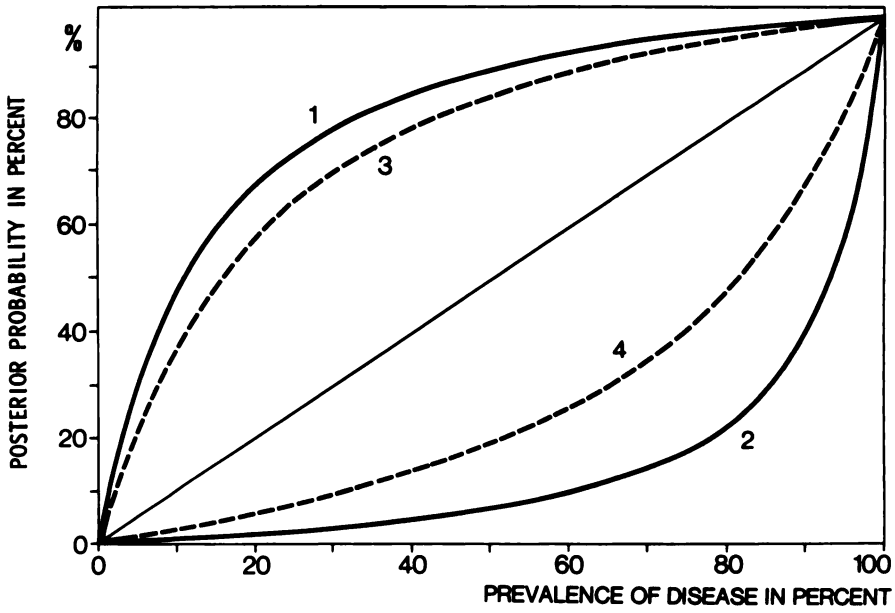

(1) posterior probability of true positive SPECT-scan
(2) posterior probability of false negative SPECT-scan
(3) posterior probability of true positive conventional scintigram
(4) posterior probability of false negative conventional scintigram

FIG. 4. Bayesian analysis applied to decision matrix shown in Table 2. It shows that probabilities of true positives and false negatives with both SPECT and conventional scintigrams are dependent on prevalence of disease.

The classification of lesions according to size and location demonstrated that SPECT's sensitivity was lowest for small lesions in the middle third of the liver. The location of the lesions appeared to be of particular importance since SPECT, unlike TCT, fails to provide information about anatomic landmarks. Metastases may be suggested by circumscribed defects resulting from impressions of the kidney or the gallbladder. It does appear that SPECT will detect defects most effectively in the right-hand third of the liver, since some large lesions were missed in the left-hand third. This occurred when the left lateral border of the liver was not correctly recognized. Small defects located beneath the hilus were easily missed, resulting in considerable loss of sensitivity in this area.

Respiratory movement influences imaging. The hepatic movement during respiration at rest is approximately 1.3 cm (*14*). Different approaches have been

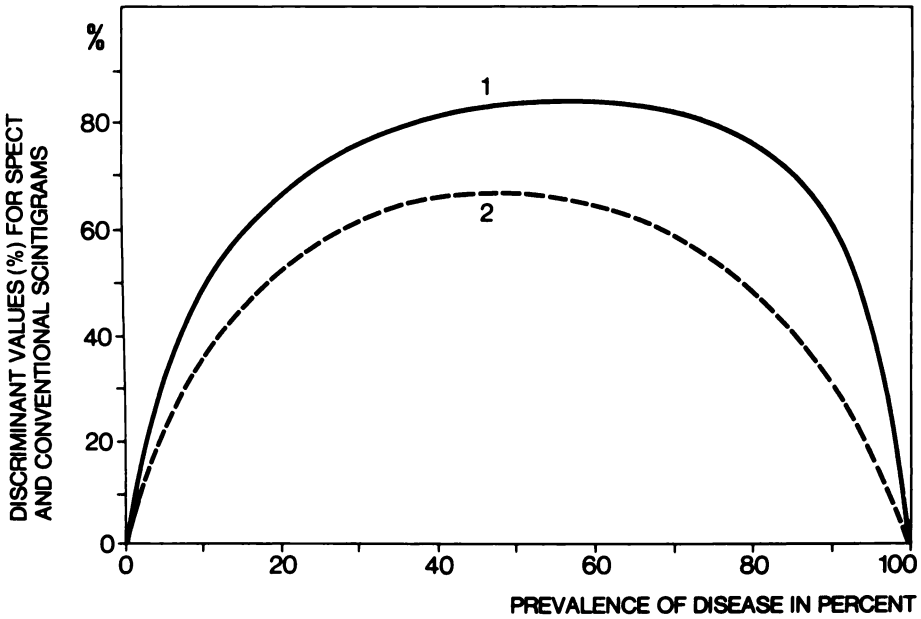

(1) discriminant curve of SPECT
(2) discriminant curve of conventional scintigram

FIG. 5. Discriminant curves calculated from results of 130 examinations. Discriminant values were obtained by calculating difference between true positives and false negatives found with SPECT or with conventional scintigraphy. Discriminant values are dependent on disease prevalence.

devised to correct for the liver's respiratory motion (*15–19*). The scintigraphic detection of focal defects could be improved with motion correction (*15–16,20*). Further image improvement may be achieved by increasing the average count rate. We prefer average image count rates of 150,000 to 200,000 counts. Collimators with improved depth resolution would further increase small-lesion detection.

The comparison of TCT diagnosis with the results of SPECT and conventional imaging showed that SPECT is clearly the superior scintigraphic modality. Nevertheless, resolution below 2 cm was poor. The high sensitivity of SPECT makes it obvious that most of the patients in this study had both small and larger lesions at the same time. The relatively low sensitivity of SPECT in the detection of small lesions thus failed to influence results greatly.

Reports on the sensitivity and specificity of conventional scintigraphy are conflicting (*5–6,21–23*). Sensitivity and specificity are reported to be as low as 70% and as high as 96% (*4–5,21–22,24*). Lunia et al. reviewed 1,424 liver studies and obtained a sensitivity of 83%, specificity of 75%, and accuracy of 77% (*21*). Larsson reported a true-positive rate of 82% for SPECT, with a true-negative value of 90% (*8*). Frick et al. also demonstrated that superior results are obtained with SPECT relative to those of conventional scintigrams (*23*).

Bayesian analysis was used to compare SPECT with conventional scintigraphy at different prevalences of metastatic disease. Conventional scintigraphy achieved 80% posterior probability of disease at 42% disease prevalence, while SPECT reached this posterior probability at a 32% disease rate. Similar differences were found when the false-negative rate of the two gamma-imaging procedures were compared. The superiority of SPECT was also evident when the maximum discriminant values of the two scintigraphic procedures were compared. Conventional scintigraphy achieved a value of 66% at 48% incidence of disease, whereas SPECT achieved a value of 84% at 57% disease prevalence. These calculations suggest that SPECT can be expected to have a greater sensitivity than conventional imaging, and a lower rate of false-negatives, even at higher rates of disease prevalence.

It appears useful to compare the scintigraphic results obtained in this study with previously reported data on sensitivity and specificity of TCT. Snow et al. evaluated 94 TCT liver examinations and compared them with the results of invasive diagnostic procedures. For TCT they found a sensitivity of 96% and specificity of 86% (*4*). The false-positive ratio was 12%, the false-negative ratio 4%. Subjecting Snow's data to Bayesian analysis, we obtained the data shown in Table 4.

The prior probability of disease for obtaining an 80% posterior probability of the presence of metastasis and a positive test is similar for both SPECT and TCT. It also becomes evident that SPECT and TCT have a similar frequency of false-negatives at the 80% true-positive level.

TABLE 4. RESULTS OF SPECT AND CONVENTIONAL SCINTIGRAPHY ARE COMPARED TO SNOW'S FINDINGS IN 94 TCT EXAMINATIONS.*

	Prior probability of metastasis for 80% posterior probability of disease	False-negative rate of 80% posterior probability of disease
Conventional scintigraphy (this study)	42%	14%
SPECT (this study)	32%	3%
TCT (Snow et al)	33%	2%

* All data were subjected to Bayesian analysis. The prior probability of metastatic involvement needed for 80% posterior probability of disease is calculated. The false-negative rate for this posterior probability was also determined.

In conclusion, the low frequency of false-negatives obtained with SPECT suggest that the procedure is more effective than conventional scintigraphy at low disease prevalence. SPECT should therefore find preferential use in ruling out hepatic involvement in a patient with malignant disease.

APPENDIX

1. The assessment of SPECT and conventional imaging was based on the following general decision matrix:

For SPECT

SPECT	TCT pos	TCT neg
pos	a	c
neg	b	d

For conventional scintigraphy

CONVENTIONAL SCAN	TCT pos	TCT neg
pos	a	c
neg	b	d

Sensitivity [a/(a + b)], specificity [d/(c + d)] and accuracy [(a + d)/(a + b + c + d)] were calculated for both conventional imaging and SPECT.

2. The sensitivity (true-positive ratio) of SPECT was calculated for each group of lesions with a definite diameter using the formula:

$$TP(i) = a(i)/[a(i) + b(i)]$$

i: is a group of lesions with a definite diameter as determined by TCT.

a(i): the number of visible Group i defects in SPECT and TCT.
b(i): the number of missed Group i lesions in SPECT, identified in TCT.
a(i) + b(i): the sum of Group i defects seen by TCT.
TP(i): the true-positive ratio (sensitivity) of Group i.

3. The same calculations were carried out for lesions classified according to location.

4. The Bayesian theorem was used to assess the utility of the two scintigraphic procedures at different disease prevalences.

a) The equation used to calculate the posterior probability of having metastases when SPECT, or the conventional scintigram, was abnormal was:

$$P1 = \{a/(a + b)\}P(D+)/[\{a/(a + b)\}P(D+) + \{c/(c + d)\}P(D-)]$$

where P(D+) is the prior probability of having metastatic disease (in percent), and P(D−) is 100 − P(D+).

b) The posterior probability of having metastases when SPECT, or the conventional scintigram, was normal was calculated using the equation:

$$P2 = \{b/(a + b)\}P(D+)/[\{b/(a + b)\}P(D+) + \{d/(c + d)\}P(D-)]$$

c) P(D+) was varied from 0 to 100% in Eqs. 4a and 4b. If a, b, and c are considered to be constant, the resulting curve demonstrates the relationship between prevalence and posterior probability. Since a, b, and c are constants without standard deviation, no error bars are obtained. The discriminant value was calculated for all prevalences of disease [P(D+)] as follows:

$$F(j) = P1(j) - P2(j) \text{ for all prevalences } j.$$

d) The P(max) value was used to determine the prevalence of disease by obtaining the maximum F-value

$$P(max) = \frac{1}{1 + \sqrt{\left[\frac{b}{a+b} \cdot \frac{a}{a+b}\right] \div \left[\frac{d}{c+d} \cdot \frac{c}{c+d}\right]}} = \frac{1}{1 + \frac{c+d}{a+b}\sqrt{ab/cd}}$$

ACKNOWLEDGMENT

We thank Mr. Hans-Jürgen Adrian and Miss Heike Streib for their expert technical assistance. We also thank Mrs. Ellen Bender for her help in preparing the manuscript. The camera (GE 400 T) was given for this study by General Electric Corp.

REFERENCES

1. MANGUM JF, POWELL MR: Liver scintiphotography an index of liver abnormality. *J Nucl Med* 14:484-489, 1973
2. TAYLOR KJW, ROSENFIELD AT: Grey-Scale ultrasonography in the differential diagnosis of jaundice. *Arch Surg* 112:820-825, 1977
3. ROBBINS AH, PUGATCH RD, GERZOF SG, et al: Observations on the medical efficacy of computed tomography of the chest and abdomen. *Am J Roentgenol* 131:15-19, 1978
4. SNOW JH, GOLDSTEIN HM, WALLACE S: Comparison of scintigraphy, sonography, and computed tomography in the evaluation of hepatic neoplasms. *Am J Roentgenol* 132: 915-918, 1979
5. SCHERER U, BÜLL U, ROTHE R, et al: Computerized tomography and nuclear imaging of the liver: a comparative study in 83 cases. *Eur J Nucl Med* 3:71-80, 1978
6. SCHERER U, ROTHE R, EISENBURG J, et al: Diagnostic accuracy of CT in circumscript liver disease. *Am J Roentgenol* 130:711-714, 1978
7. JASZCZAK RJ, COLEMAN RE, WHITEHEAD FR: Physical factors affecting quantitative measurements using camera-based single photon emission computed tomography (SPECT). IEEE Transactions on Nuclear Science, Vol. NS-28. No. 1, 1981, pp 69-80
8. LARSSON SA: Gamma camera emission tomography. *Acta Radiol* (Suppl 363):1-75, 1980
9. JASZCZAK RJ, CHANG LT, STEIN NA, et al: Whole-body single-photon emission computed tomography using dual, large-field-of-view scintillation cameras. *Phys Med Biol* 24:1123-1143, 1979
10. SHEA G: An analysis of the Bayes' Procedure for diagnosising multistage diseases. *Comput Biomed Res* 11:65-75, 1978
11. SONNENBERG A: Bayessches Theorem bei klinischer Differentialdiagnose. *Dtsch Med Wschr* 103:1443-1447, 1978
12. MURRAY RG, MCKILLOP JH, BESSENT RG, et al: Bayesian analysis of stress thallium-201-scintigraphy. *Eur J Nucl Med* 6:201-204, 1981
13. SCHERER U, SANTOS M, LISSNER J: CT studies of the liver in vitro: A report on 82 cases with pathological correlation. *J Comput Assist Tomogr* 3:589-595, 1979
14. WEISS PH, BAKER JM, PATCHEN EJ: Assessment of hepatic respiratory excursion. *J Nucl Med* 13:758-759, 1972
15. HARAUZ G, BRONSKILL MJ: Comparison of the liver's respiratory motion in the supine and upright positions: Concise communication. *J Nucl Med* 20:733-735, 1979
16. BAIMEL NH, BRONSKILL MJ: Optimization of analog-circuit motion correction for liver scintigraphy. *J Nucl Med* 19:1059-1066, 1978
17. DELAND FH, MAUDERLI W: Gating mechanism for motion-free liver and lung scintigraphy. *J Nucl Med* 13:939-941, 1972
18. ELINGS VB, MARTIN CB, POLLOCK IG, et al: Electronic device corrects for motion in gamma camera images. *J Nucl Med* 15:36-37, 1973
19. SCHMIDLIN P: Development and comparison of computer methods for organ motion correction in scintigraphy. *Phys Med Biol* 20:465-476, 1975
20. TURNER DA, FORDHAM EW, ALI A, et al: Motion corrected hepatic scintigraphy: An objective clinical evaluation. *J Nucl Med* 19:142-148, 1978
21. LUNIA S, PARTHASARATHY KL, BAKSHI S, et al: An evaluation of ^{99m}Tc-Sulfur colloid liver scintiscans and their usefulness in metastatic workup: A review of 1,424 studies. *J Nucl Med* 16:62-65, 1974
22. DRUM DE, CHRISTACOPOULOS JS: Hepatic scintigraphy in clinical decision making. *J Nucl Med* 13:908-915, 1972
23. FRICK MP, KNIGHT LC, PONTO RA, et al: Evaluation of three imaging instruments in dogs with liver hematomas: Concise communication. *J Nucl Med* 20:448-449, 1979
24. OSTER ZH, LARSON SM, STRAUSS HN, et al: Analysis of liver scanning in a general hospital. *J Nucl Med* 16:450-453, 1974